ACS APPLIED MATERIALS & INTERFACES

Research Article

www.acsami.org

Highly Conductive and Low Cost Ni-PET Flexible Substrate for Efficient Dye-Sensitized Solar Cells

Haijun Su,*[,†,‡,∥] Mingyang Zhang,[†,∥] Ya-Huei Chang,[†] Peng Zhai,[†] Nga Yu Hau,[†] Yu-Ting Huang,[†] Chang Liu,[†] Ai Kah Soh,[†,§] and Shien-Ping Feng*[,†]

[†]Department of Mechanical Engineering, The University of Hong Kong, Hong Kong

[‡]State Key Laboratory of Solidification Processing, Northwestern Polytechnical University, Xi'an, 710072 Shaanxi, P. R. China

[§]Monash University Sunway Campus, 46150 Petaling Jaya, Selangor, Malaysia

Supporting Information

ABSTRACT: The highly conductive and flexible nickel-polyethylene terephthalate (Ni-PET) substrate was prepared by a facile way including electrodeposition and hot-press transferring. The effectiveness was demonstrated in the counter electrode of dye-sensitized solar cells (DSSCs). The Ni film electrodeposition mechanism, microstructure, and DSSC performance for the Ni-PET flexible substrate were investigated. The uniform and continuous Ni film was first fabricated by electroplating metallic Ni on fluorine-doped tin oxide (FTO) and then intactly transferred onto PET via hot-pressing using Surlyn as the joint adhesive. The obtained flexible Ni-PET substrate shows low sheet resistance of 0.18Ω/□ and good chemical stability for the I^-/I^{3-} electrolyte. A high light-to-electric energy conversion efficiency of 7.89% was demonstrated in DSSCs system based on this flexible electrode substrate due to its high conductivity, which presents an improvement of 10.4% as compared with the general ITO-PEN flexible substrate. This method paves a facile and cost-effective way to manufacture various metals on a plastic nonconducive substrate beneficial for the devices toward flexible and rollable.

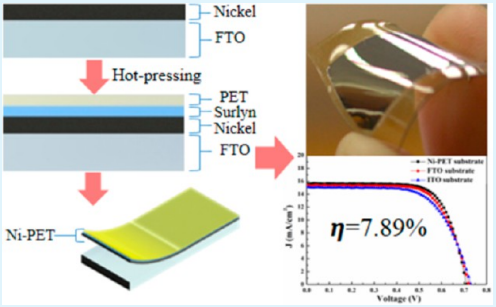

KEYWORDS: *flexible substrate, counter electrode, electrodeposition, conductive, photovoltaic, dye-sensitized solar cell*

1. INTRODUCTION

As a promising alternative for next generation of renewable green energy, dye-sensitized solar cells (DSSCs) have attracted great attention due to their low cost, environmental friendliness, simple fabrication, great potential of miniaturization, and portability,[1−4] as well as the recent high power conversion efficiency up to 12% on fluorine-doped tin oxide (FTO) glass substrates.[5] In general, DSSCs are composed of transparent conductive oxide (TCO) glass substrates, dye-sensitized TiO_2 thin film, liquid redox electrolyte, and platinum (Pt) counter electrode (CE),[1] in which the TCO glass substrates extremely account for the cells volume, weight, and cost (~60%).[6] Moreover, as noted, TCO glass is fragile and rigid, whose shape greatly limits its roll-to-roll mass production. As a result, toward the future where DSSCs go rollable and lightweight,[7,8] indium tin oxide (ITO) fabricated on plastic substrate has been widely developed.[4,8,9] Contrary to the rigid glass substrate, the polymeric substrates, such as polyethylene naphthalate (PEN) and polyethylene terephthalate (PET), cannot withstand the high temperature so that ITO has to be coated by using RF or DC magnetron sputtering at low temperature (<150 °C).[8,10,11] Consequently, the ITO-PEN generally presents a relatively high sheet resistance (15−30 Ω/□) and poor wettability,[8] degrading the performance of flexible DSSCs. Additionally, the fabrication process of ITO substrate is time-consuming and requires costly vacuum equipment.[12−14] Accordingly, a cost-effective flexible substrate, which possesses low sheet resistance, economic efficiency, good chemical stability, and high electrocatalytic activity for the reduction of the I_3^-/I^- redox couple, will be greatly beneficial to facilitate DSSCs toward flexible and rollable.[15−17]

Many groups have devoted their efforts to reduce the preparation cost of currently used ITO-PEN or develop a new flexible substrate.[18−25] Recently, the low temperature solution-based processes to fabricate ITO film on plastic substrates have been developed,[18−21] but the resistance is relatively high due to the unavoidable impurities remaining in the finished layer. As compared with ITO, metal films have superior conductivity. Therefore, the aqueous methods to coat metal thin film on plastic substrates present greater potentials due to their low cost and low resistance, thereby attracting considerable research interest.[22−26] Takehiro et al. fabricated a conductive substrate by using the self-assembly of Ag nanowires in a bubble template.[24] Chen et al. coated Ag thin films on PET sheets by inkjet-printing a self-reduction silver ink synthesized by silver ammonia solution mixed with diethanolamine (DEA).[25]

Received: December 30, 2013
Accepted: March 26, 2014
Published: March 26, 2014

   dx.doi.org/10.1021/am406026n | ACS Appl. Mater. Interfaces 2014, 6, 5577−5584

However, their applications as a flexible counter electrode substrate in DSSCs have not been reported. Moreover, the fabrication processes involve many steps, and silver is easily dissolved into the iodide-based electrolyte.[27] Recently, graphene has been studied to replace Pt-based flexible CEs but requires a costly fabrication process. In addition, the reduction electrocatalytic activities of the flexible graphene-based CEs still cannot match up to those of Pt so that limits their further applications.[28,29]

In this work, we therefore aim to develop a highly conductive and flexible Ni-PET substrate prepared by a facile solution electrodeposition and film-transferring approach, which is demonstrated as a flexible substrate in DSSCs CE. Ni-PET has a high electrical conductivity, good chemical stability, and low cost[30] as well as good flexibility. The polyvinylpyrrolidone (PVP)-capped Pt nanoparticles (PtNPs) were coated on the Ni-PET substrate by a two-step dip coating process at low temperature to fabricate highly conductive PtNPs/Ni-PET CE. The DSSCs with the Ni-PET substrate show a superior energy conversion efficiency of 7.89% compared to the general ITO-PEN substrate and the rigid FTO substrate. The developed method is expected to provide a cost-effective and high-performance flexible substrate to facilitate DSSCs toward flexible, rollable, and lightweight.

2. EXPERIMENTAL SECTION

2.1. Preparation of Conductive Ni-PET Flexible Substrate. The FTO glasses with size of 1 × 3 cm^2 (7Ω/□, 2.2 mm thick, Pilkington) were ultrasonically cleaned in 4% glass cleaner (PK-LCG545, Parker) at 50 °C for 30 min, followed by rinsing with deionized water. The electrodeposition of Ni was carried out in a standard three-electrode system by using the FTO glass as the working electrode, a clean Pt mesh as the counter electrode, and an Ag/AgCl electrode as the reference electrode. Nickel was then electroplated onto the Bepop mask (Max, CM-200E) covered FTO glass under a constant operating voltage (−2 V) from a commercial electrolyte (Electroless Nickel Jumbo Kit, CASWEL) at 53 °C.[29] Meanwhile, PET (200 μm thick, XinRuiDa) plastic with the size of 1.5 × 2 cm^2 was cleaned, dried, and then treated by UV ozone (350 nm, TK-110-H01, Kingo). The Ni-PET flexible substrate was then obtained by transferring the electroplated Ni film from FTO to the PET surface via hot pressing under 140 °C for 30 s using a Surlyn (Surlyn 1706, DuPont) as the joint adhesive, as schematically shown in Figure 1.

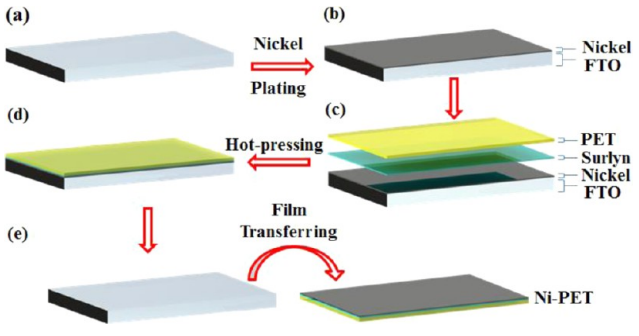

Figure 1. The schematical process flow for fabrication of a conductive Ni-PET flexible substrate. (a) A FTO glass was ultrasonically in glass cleaner and rinsed with deionized water; (b) The metallic nickel layer was electroplated on FTO glass; (c) The electroplated Ni film was transferred to a PET surface by hot-pressing, and Surlyn was worked as the joint adhesive, creating the Ni-PET layer on the FTO substrate (d); (e) The Ni-PET substrate was removed from the FTO substrate to obtain a conductive Ni-PET flexible substrate.

Two holes with diameters of 0.5 mm were drilled by a drilling machine so as to inject an electrolyte during DSSCS assembly.

2.2. Preparation of Flexible PtNPs/Ni-PET CE. A two-step dip-coating process was utilized to prepare PtNPs/Ni-PET CE. Ni-PET was first immersed in a 1% conditioner solution (ML-371, OM Group) for 5 min at 60 °C to change the surface charge state of the substrate to facilitate PtNPs adsorption and then was treated in PVP-PtNPs suspension (250 ppm, ACROS) for 10 min at 40 °C to form a thin catalytic Pt layer. The preparation of PVP-PtNPs solution can refer to our previous paper.[31] After each step, the substrate was rinsed with deionized water and dried using high-pressure nitrogen. UV (275W, TK-110-H01, Kingo) was used for 10 min to decompose the capped PVP to obtain PtNPs/Ni-PET CE. As the references, the PtNPs/FTO glass CE and PtNPs/ITO-PEN flexible CE were also prepared with the same method for the comparison.[28]

2.3. Fabrication of DSSCs. The 1.5 cm × 1.5 cm FTO glass (10Ω/□, 3.1 mm thick, Nippon Sheet Glass) was used as the photoanode substrate. The commercial nano-TiO_2 paste (particle size 20 nm, Eternal) was coated on the cleaned FTO glass by screen printing to form a film with 10 μm thickness, and then a 4 μm TiO_2 film was printed on it as a light scattering layer using another TiO_2 paste (PST400, CCIC). The resulting TiO_2 bilayer film was sintered at 450 °C for 30 min to remove the organics and then slowly cooled to room temperature. Subsequently, the sintered TiO_2 photoanode was immersed in a 0.4 mM N719 dye solution (Solaronix) at room temperature for 12 h in order to sufficiently absorb dye molecules, followed by rinsing with ethanol and drying in air. The DSSCs were fabricated by sandwiching TiO_2 photoanode (FTO-based) and flexible PtNPs/Ni-PET CE with an electrolyte (0.2 M PMII, 0.05 M I_2, 0.1 M LiI, 0.2 M TBAI, 0.5 M, TBP in AN/VN) using a 25 μm thick thermal-plastic Surlyn spacer (SX1170-25, Solaronix). The active area of the cells is 0.16 cm^2. Finally, the injection holes were hot sealed using a piece of thin cover glass with a hot-melt film underneath as an adhesive. For comparison purposes, the DSSCs based on PtNPs/FTO CE and PtNPs/ITO-PEN CE with the same photoanodes were assembled.

2.4. Characterization. The voltage and current of Ni deposition was determined by measuring the linear sweep voltammetry (LSV) from −0.5 to −2.5 V at a scanning rate of 5 mV/s. The Ni plating current versus time (chronoamperometry) at constant voltage was measured. The surface morphology and composition of the as-plated Ni and PtNPs/Ni-PET were investigated by field-emission scanning electron microscope (SEM, S-4800, Hitachi) and energy dispersive X-ray spectrometer (EDS). The four-point probe method was used to measure the surface resistance. The electrochemical impedance spectroscopy (EIS) was measured by scanning the symmetric dummy cell (CE/electrolyte/CE) with a potentiostat (CHI 660E) from 100 kHz to 0.1 Hz with 5 mV amplitude at open-circuit conditions. The photocurrent−voltage (J-V) curves of DSSCs were recorded with a computer-controlled digital source meter (Keithley 2400) under exposure of a standard solar simulator (PEC-L01, Pecell) under 1 sun illumination (AM 1.5G, 100 mW cm^{-2}) based on four cells for each condition.

3. RESULTS AND DISCUSSION

3.1. Electrodeposition Behavior of Nickel Films on FTO. It is known that the electroplating is a simple and cost-effective method to prepare metallic film on the conductive substrate, which has been widely used in various fields. Ni is a highly conductive metal commonly used in microelectronic and optoelectronic devices. It has been reported that Ni also has high stability against corrosive liquid electrolyte when used in the DSSCs.[32,33] However, the PET plastic is nonconductive, which is not allowed to directly deposit Ni particles on it. To resolve this issue, a facile approach including electrodeposition and film-transferring was used, which first obtained a metallic film on a FTO substrate and then transferred the metallic film onto the PET substrate. As noted, different from the common

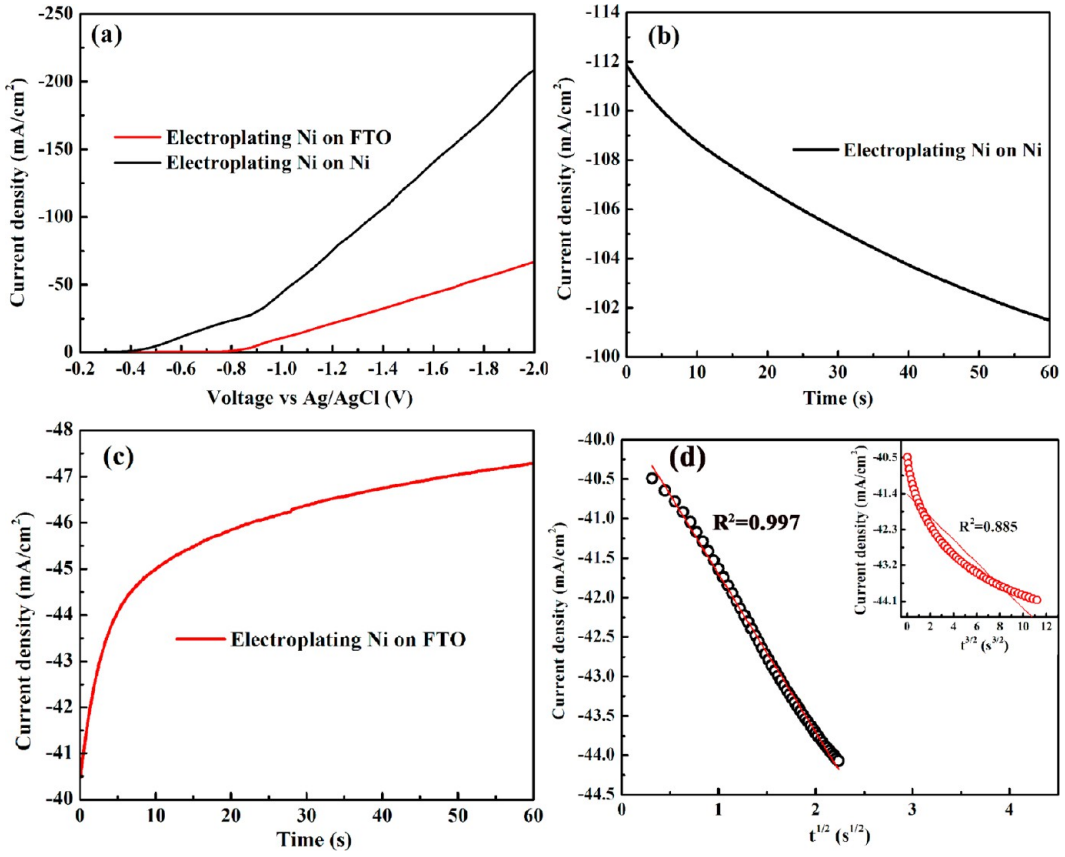

Figure 2. Linear sweep voltammetry for Ni electroplated on a Ni plate and FTO at a potential scan rate of 5 mV/s (a); Chronoamperograms of electroplating Ni on a Ni plate (b) and FTO (c) under an operating voltage of −2 V; (d) Dependence of i vs $t^{1/2}$ plot for the initial transient portion of Ni electroplated on FTO. The inset shows the dependence of i vs $t^{3/2}$ plot.

electrodeposition,[34] it requires a dense Ni film having a relatively poor adhesion on FTO so as to peel off the intact Ni film from FTO surface. In this case, the nucleation process of electroplated nickel on FTO is of importance to determine the Ni film quality and its adhesion.

Figure 2a shows the typical LSV curves of Ni electroplated on Ni and FTO substrates from commercial Ni electrolyte at 53 °C based on a potential scan rate of 5 mV/s. During the electroplating process, the film generally undergoes the processes of nucleation (due to deposition potential) and growth (due to current density). As seen, the I−V curve of nickel on the FTO glass presents a more negative shift (−0.8 V) than the Ni plate (−0.4 V), which indicates that the nickel electrodeposition onto the FTO surface requires a higher nucleation energy. This means that the films deposited on FTO prefer to form poor adhesion than on the Ni plate, which is more favorable to later film-transferring. The chronoamperograms (Figure 2b and c) display the current response at an optimized operating voltage of −2 V for Ni electroplated on Ni and FTO. As seen, the current response of electroplating Ni on Ni is correlated with the Cottrell equation, which reveals a certain amount of nucleation sites are rapidly generated in the very beginning and then gradually reach a diffusion control (Figure 2b). In the case of electroplating Ni on FTO, the current response increases at an initial few seconds and then reaches a plateau (Figure 2c). As noted, the current density of electroplating Ni on FTO is about two times lower than that on Ni. The reason is that the relatively poor wettability (low surface energy) of FTO leads to a higher nucleation energy so that Ni atoms are more preferably bound to each other than to the FTO surface.[35] As shown in Figure 2d, the initial transient portions of the experimental data were analyzed in i vs $t^{1/2}$ plot for the characterization of instantaneous nucleation, while i vs $t^{3/2}$ plot in the inset for the progressive nucleation. A good linearity in i vs $t^{1/2}$ plot indicates that an instantaneous nucleation occurs when electroplating Ni on FTO. In the case of instantaneous nucleation, the nuclei density is almost the same as the initial nuclei density (N_0), which can be calculated based on the following equation[36]

$$N_0 = 0.065(8\pi CM/\rho)^{-1/2}[zFC/(i_{max}t_{max})]^2 \quad (1)$$

where C is the metal ion concentration in the solution, zF is the molar charge transferred during electrodeposition, i_{max} is the peak current density, t_{max} is the peak time, and M and ρ are molecular weight and density of the deposited material, respectively. The calculated nuclei density of nickel on FTO is around 1.7×10^7 cm^{-2}, which is much smaller than the general value of the nuclei density (~10^9 cm^{-2}) for electroplating Ni on metal substrates.[37] The average rate of Ni film deposition on FTO is about 0.8 μm/min based on the measured film thickness by the α-step method (Figure S1).

Figure 3 shows the SEM microstructure morphology of electroplated nickel on a blank FTO at −2 V for different initial electrodeposition times of 0, 0.25, and 0.5 s. As seen, the blank FTO glass exhibits an uneven and random distribution of tin oxide grains with an obvious grain boundary and irregular shape and large size (Figure 3a). After an instantaneous deposition of 0.25 s, spherical Ni nuclei with a adiameter size of about 40 nm

dx.doi.org/10.1021/am406026n | ACS Appl. Mater. Interfaces 2014, 6, 5577−5584

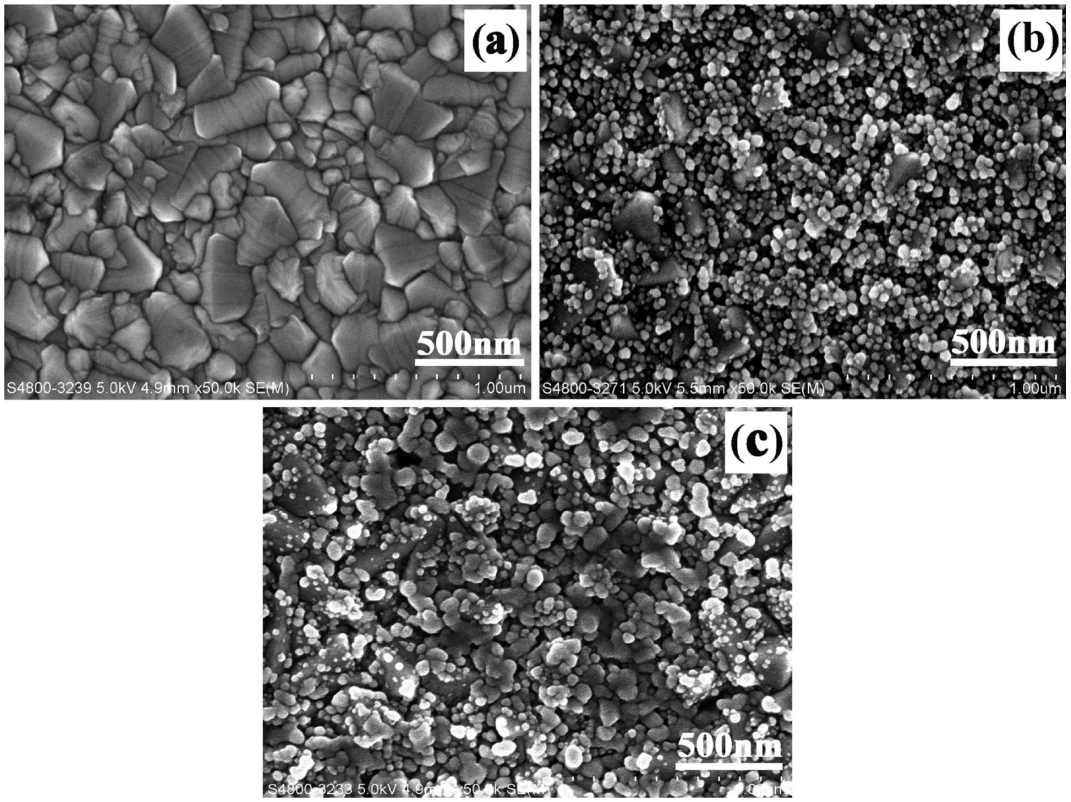

Figure 3. SEM images showing the microstructure morphology of electroplated nickel on blank FTO at an initial deposition time of 0 s (a), 0.25 s (b), and 0.5 s (c) at an operating voltage of −2 V.

have been formed (Figure 3b). With further increasing the deposition time (Figure 3c), it is found that the number of nucleation sites does not increase, but the sizes of particles increase and the distributions of size and shape become uneven. In this stage, the formation of Ni nuclei has finished, and Ni grain begins to grow, of which the growth rate is determined by the operating current. As mentioned, the early stage of the electrochemical phase transformation corresponds to an instantaneous nucleation model, where the growth of nuclei on a small number of active sites, such as atomic step, grain edge, crystal defects, and impurities,[31] occurs in a very short time period. These nucleation sites grow into islands and then coalesce (Volmer−Weber growth).[38,39] Island growth during electroplating nucleation is usually not desirable for technological applications due to its poor adhesion. Here, in contrast, we utilized this unique property to transfer the intact Ni film from FTO to PET via hot-pressing with the aid of Surlyn as a joint adhesive. The peel-off test demonstrates that the nickel film can be simply and intactly detached from FTO by an ordinary tape due to its weak interfacial adhesion, as seen in Figure 4.

3.2. Characterization of Ni-PET and PtNPs/Ni-PET Substrates. Figure 5a shows the SEM microstructure morphology of the obtained flexible Ni-PET. The composition of the film is characterized by EDS (Figure S2) and listed in Table 1. As seen, the morphology of the Ni surface is an inverse morphology of the FTO surface because electroplated Ni was grown along with FTO. It provides a microroughness Ni surface which is beneficial to the subsequent two-step PVP-PtNPs dip-coating process.[10] As shown in Figure 5b, the Pt nanoclusters are homogeneously distributed on the surface of Ni-PET. Compared with PtNPs/FTO and PtNPs/ITO-PEN

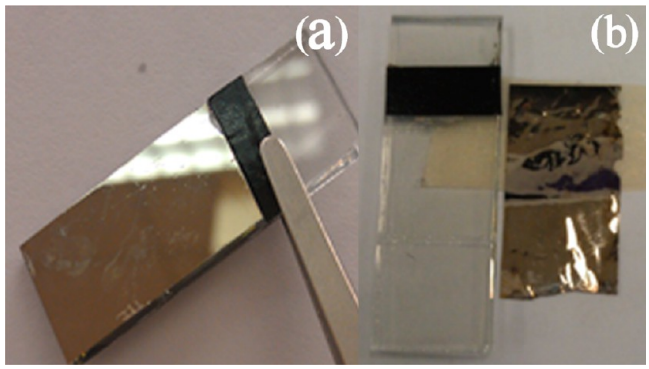

Figure 4. Typical photograph (a) of electroplated nickel on blank FTO at an operating voltage of −2 V for 60 s. (b) Showing the film is completely peeled off by the tape.

using the same coating process (Figure S3), the relatively high Pt loading of 1.64 wt % can be achieved in PtNPs/Ni-PET (Table 1). Moreover, no significant carbon impurity was found on PtNPs/Ni-PET (Figure S4), revealing that most of PVP can be completely decomposed by UV treatment.

As mentioned, Surlyn plays an important role to joint Ni and PET together via hot pressing. In this sandwich scheme, the adhesion between Surlyn and PET is not as good as that between Surlyn and Ni, causing a localized peeling under bending deformation, as shown by the red circles in Figure 6a. To solve this problem, UV ozone treatment was employed to modify the PET surface before hot pressing to enhance the interfacial bonding. Figure 6b shows no obvious peeling or cracks occurring under bending deformation. The sheet resistance of the Ni-PET substrate is 0.18 Ω/□ measured by

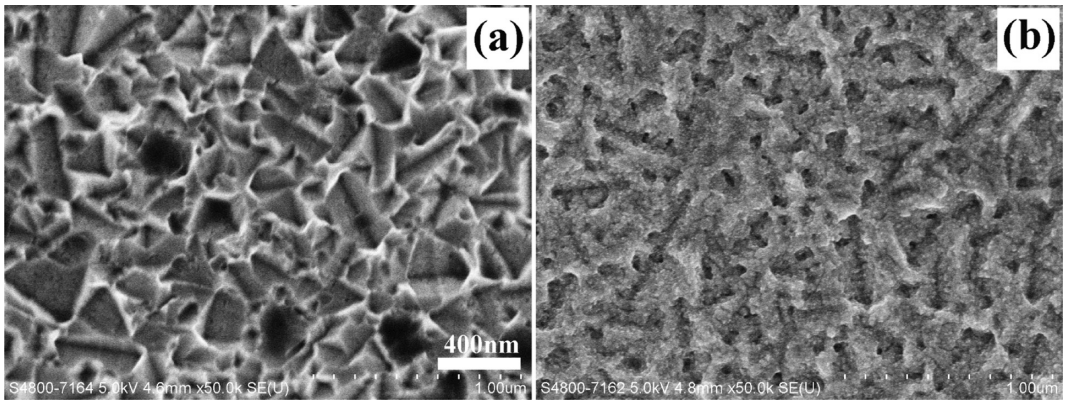

Figure 5. SEM images showing the microstructure morphology of the transferred Ni-PET film (a) and the PtNPs/Ni-PET film (b).

Table 1. Composition of Ni-PET and PtNPs/Ni-PET Films

film	element	weight percent (wt %)	atomic percent (at %)
Ni-PET	Ni	100.00	100.00
PtNPs/Ni-PET	Ni	98.36	99.50
	Pt	1.64	0.50

the four-point probe method, which is obviously superior to FTO (10 Ω/□) and ITO-PEN (15−30 Ω/□).[40] This result indicates that the obtained Ni-PET film possesses high conductivity and good bending characteristics, which is suitable to be used as DSSCs CE.

3.3. Photovoltaic Performance of DSSCs. The interfacial electrochemical behaviors between flexible Pt/Ni-PET CEs and electrolytes are determined by a two-electrode EIS system. For comparison purposes, three kinds of CEs (PtNPs/Ni-PET, PtNPs/ITO-PEN, PtNPs/FTO) were investigated. Here, these eletrodes were all assembled with another PtNPs/FTO and thereby formed the symmetric (PtNPs/FTO vs PtNPs/FTO) or the asymmetric (PtNPs/Ni-PET vs PtNPs/FTO or PtNPs/ITO-PEN vs PtNPs/FTO) two-electrode dummy cells. The Nyquist plots of three dummy cells are shown in Figure 7a. The equivalent circuit is depicted in the inset of Figure 7a including series resistance (R_s) in the high-frequency region, charge transfer resistance (R_{ct}) and double-layer capacitance (C_{ct}) in the middle frequency region, and electrolyte diffusion resistance (Z_w) in the low frequency.[41] Resistance contribution of each CE in the symmetric cell (FTO/FTO) can be simply divided by two, while that in the asymmetric cases (Ni-PET/FTO, ITO-PEN/FTO) should be obtained by subtracting the resistance of single PtNPs/FTO from the total resistance. The fitted data based on this model is summarized in Table 2. As seen, PtNPs/Ni-PET CE shows a much smaller R_s of 0.23 Ω than PtNPs/FTO CE of 7.48 Ω and PtNPs/ITO-PEN CE of 12.94 Ω, which is mainly attributed to the low sheet resistance of the Ni film. The great decrease of R_s is beneficial to enhance the electron transportation ability and thereby to improve the fill factor of DSSCs.[42]Based on the first semicircles (Figure 7a), the charge transfer resistances for these CEs are almost the same, indicating the similar electrochemical catalytic activity to the I^{3-}/I^- redox reaction. The electrolyte diffusion resistance (Z_w) represented in the second semicircles shows a slight increase in PtNPs/Ni-PET CE compared to its counterparts possibly due to the localized relative long diffusion distance coming from the inverse FTO microstructure (see Figure 5). Meanwhile, the catalytic peaks (Figure 7b) for three counters lie at the same frequency, revealing that the flexible Pt/Ni-PET CE performs a good catalytic activity comparable to Pt/FTO CE and Pt/ITO-PEN CE. Moreover, the corresponding Bode

Table 2. Electrochemical Impedance Parameters of the Two-Electrode Configuration Based on the Ni-PET, FTO, and ITO-PEN Substrates

substrate	R_s (Ω)	R_{ct} (Ω)	Z_w (Ω)
Ni-PET	0.23	2.04	2.41
FTO	7.48	2.42	1.31
ITO-PEN	12.94	1.68	1.81

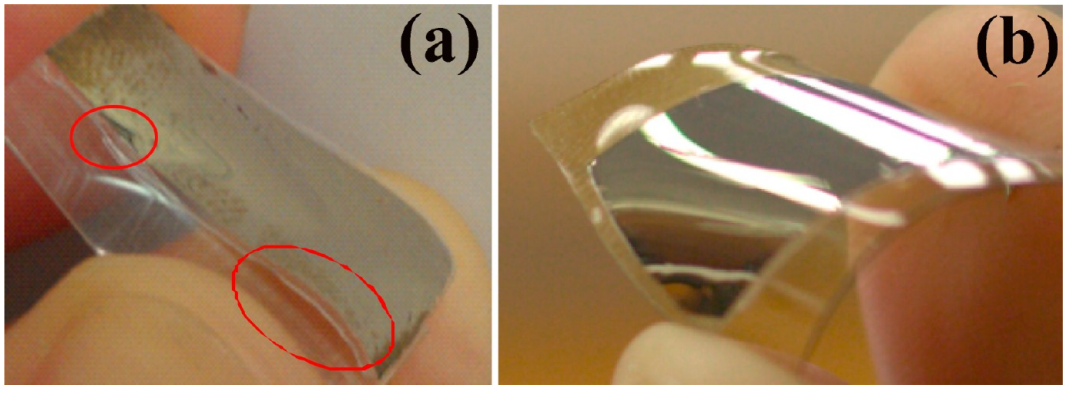

Figure 6. Photographs of the transferred nickel film onto the PET substrate during bending: (a) PET without UV ozone treatment and (b) PET with UV ozone treatment.

dx.doi.org/10.1021/am406026n | ACS Appl. Mater. Interfaces 2014, 6, 5577−5584

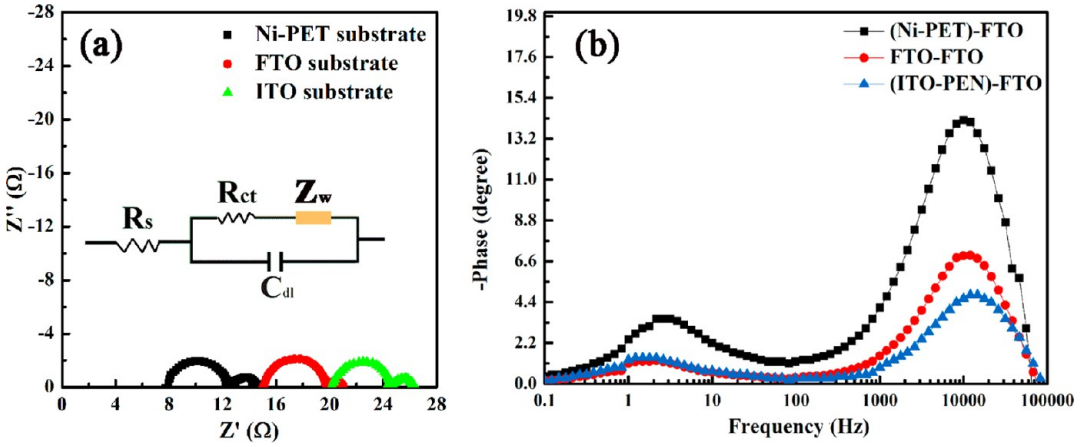

Figure 7. Nyquist plots (a) and Bode plots (b) of the dummy cells based on different CE substrates of Ni-PET, FTO, and ITO-PEN. The inset in (a) is the equivalent circuit diagram.

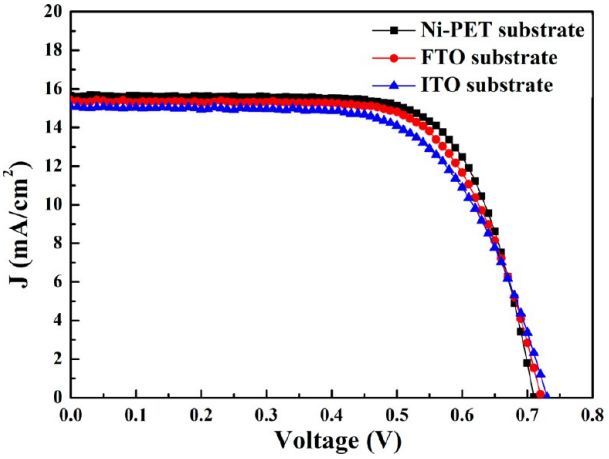

Figure 8. Photocurrent density-photovoltage (J-V) curves of DSSCs based on Ni-PET, FTO, and ITO-PEN substrates.

Table 3. Photovoltaic Performance Parameters of DSSCs Based on the Ni-PET, FTO, and ITO-PEN Substrates[a]

substrate	J_{sc} (mA cm^{-2})	V_{oc} (V)	FF	η (%)
Ni-PET	15.63 ± 1.4	0.71 ± 0.01	0.71 ± 0.07	7.89 ± 0.26
FTO	15.41 ± 0.96	0.72 ± 0.04	0.68 ± 0.03	7.59 ± 0.58
ITO-PEN	15.09 ± 2.62	0.73 ± 0.07	0.65 ± 0.05	7.15 ± 0.02

[a]The data is collected from four cells.

plot in Figure 7b shows the same level of characteristic electron lifetime constant ($\tau_e = 1/2\pi f$),[43] indicating the same reaction rate of the I^{3-}/I^- redox reaction among PtNPs/Ni-PET CE, PtNPs/ITO-PEN CE, and PtNPs/FTO CE.

Figure 8 shows the photovoltaic performance of the DSSCs based on PtNPs/Ni-PET, PtNPs/ITO-PEN, and PtNPs/FTO CEs under one sun illumination (AM 1.5 G, 100 mW/cm^2). The corresponding photovoltaic parameters are listed in Table 3. The DSSCs with PtNPs/Ni-PET CE perform a higher short circuit current density (J_{sc}) of 15.63 mA/cm^2 and an improved fill factor (FF) of 0.71 with a similar open-circuit voltage (V_{oc}) of 0.71 V in comparison with the other two CEs, resulting in a high power conversion efficiency of 7.89%. The trend of the improved short circuit current density and fill factor corresponds to the low sheet resistance of Ni-PET, consequently, achieving a 10.4% improvement of power conversion efficiency compared with DSSCs using PtNPs/ITO-PEN CE. It demonstrates that the Ni-PET based cell is not only superior to FTO or ITO-PEN based cells in the cost point of view but also in the photovoltaic performance. The properties of flexible CE are summarized in Table 4 as compared with the previous reported articles. As seen, the Ni-PET has a potential to replace FTO or ITO-PEN as a cost-effective and flexible substrate in DSSCs.

4. CONCLUSIONS

We have developed a facile and cost-effective method to fabricate highly conductive Ni-PET flexible film substrates by transferring the electroplated Ni film on PET via hot pressing. The transferred Ni-PET substrate film presents high uniformity, low sheet resistance of 0.18Ω/□, excellent scalability, and good I^-/I^{3-} electrolyte endurance. A two-step dip-coating method was utilized to prepare flexible PtNPs/Ni-PET CE to demonstrate its effectiveness in DSSCs. A high energy conversion efficiency of 7.89% is achieved based on PtNPs/Ni-PET CE, which presents an improvement of 10.4% as compared with

Table 4. Property Comparisons of the Flexible DSSC Counter Electrodes

flexible CE	preparation method	sheet resistance (Ω/□)	DSSCs efficiency (%)	reference
PtNPs/Ni-PET	electrodeposition and film-transferring	0.18 ± 0.005	7.89 ± 0.26	our work
silver nanowires/bubble template	self-assembly method	6.2	/	24
Ag/PET	inkjet-printing based on solution method	0.6	/	25
Pt/ITO-PEN	chemical reduced method	0.26−1.38Ω cm^2	5.41	10
Pt/ITO-PEN	electrodeposition method	/	6.53	37
graphene/PEDOT	modified presolution/in situ polymerization	62	6.26	28
Pt/polyester film	sputtering method	61	3.99	32
Pt/Ni sheet	sputtering method	4.6 × 10^{-4}	4.70	33

dx.doi.org/10.1021/am406026n | ACS Appl. Mater. Interfaces 2014, 6, 5577−5584

PtNPs/ITO-PEN CE and is also comparable to PtNPs/FTO CE. This facile and cost-effective method for fabricating the conductive flexible substrate has a great potential in the application of other flexible devices, such as organic solar cell and light emitted diode (LED).

■ ASSOCIATED CONTENT

Supporting Information

Thickness measurement and EDS spectrum of the Ni film on PET substrates and the SEM images and EDS results of the PtNPs/Ni-PET film. This material is available free of charge via the Internet at http://pubs.acs.org.

■ AUTHOR INFORMATION

Corresponding Authors

*E-mail: shjnpu@nwpu.edu.cn (H.S.).
*E-mail: hpfeng@hku.hk (S.P.F.).

Author Contributions

‖These authors contributed equally to this work.

Notes

The authors declare no competing financial interest.

■ ACKNOWLEDGMENTS

This work was supported by the General Research Fund from Research Grants Council of Hong Kong Special Administrative Region, China, under Award Numbers HKU 717011 and HKU 719512E and the Hong Kong Scholars Program Fund (No. XJ2011030).

■ REFERENCES

(1) O'Regan, B.; Grätzel, M. A Low-Cost, High-Efficiency Solar Cell Based on Dye-Sensitized Colloidal TiO_2 Films. *Nature* **1991**, *353*, 737−740.

(2) Grätzel, M. Photoelectrochemical Cells. *Nature* **2001**, *414*, 338−344.

(3) Grätzel, M. Recent Advances in Sensitized Mesoscopic Solar Cells. *Acc. Chem. Res.* **2009**, *42*, 1788−1798.

(4) Upadhyaya, H. M.; Senthilarasu, S.; Hsu, M. H.; Kumar, D. K. Recent Progress and the Status of Dye-Sensitised Solar Cell (DSSC) Technology with State-of-the-Art Conversion Efficiencies. *Sol. Energy Mater. Sol. Cells* **2013**, *119*, 291−295.

(5) Yella, A.; Lee, H. W.; Tsao, H. N.; Yi, C.; Chandiran, A. K.; Nazeeruddin, M. K.; Diau, E. W. G.; Yeh, C. Y.; Zakeeruddin, S. M.; Grätzel, M. Porphyrin-Sensitized Solar Cells with Cobalt (II/III)-Based Redox Electrolyte Exceed 12% Efficiency. *Science* **2011**, *334*, 629−634.

(6) Wang, Y. D.; Wu, M. X.; Lin, X.; Shi, Z. C.; Hagfeldt, A.; Ma, T. L. Several Highly Efficient Catalysts for Pt-Free and FTO-Free Counter Electrodes of Dye-Sensitized Solar Cells. *J. Mater. Chem.* **2012**, *22*, 4009−4014.

(7) Jen, H. P.; Lin, M. H.; Li, L. L.; Wu, H. P.; Huang, W. K.; Cheng, P. J.; Diau, E. W. G. High-Performance Large-Scale Flexible Dye-Sensitized Solar Cells Based on Anodic TiO_2 Nanotube Arrays. *ACS Appl. Mater. Interfaces* **2013**, *5*, 10098−10104.

(8) Weerasinghe, H. C.; Huang, F. Z.; Cheng, Y. B. Fabrication of Flexible Dye Sensitized Solar Cells on Plastic Substrates. *Nano Energy* **2013**, *2*, 174−189.

(9) Gong, Y.; Li, C. H.; Huang, X. M.; Luo, Y. H.; Li, D. M.; Meng, Q. B.; Iversen, B. B. Simple Method for Manufacturing Pt Counter Electrodes on Conductive Plastic Substrates for Dye-Sensitized Solar Cells. *ACS Appl. Mater. Interfaces* **2013**, *5*, 795−800.

(10) Chen, L. L.; Tan, W. W.; Zhang, J. B.; Zhou, X. W.; Zhang, X. L.; Lin, Y. Fabrication of High Performance Pt Counter Electrodes on Conductive Plastic Substrate for Flexible Dye-Sensitized Solar Cells. *Electrochim. Acta* **2010**, *55*, 3721−3726.

(11) Li, Y.; Cui, P.; Wang, L. Y.; Lee, H.; Lee, K.; Lee, H. Highly Bendable, Conductive, and Transparent Film by an Enhanced Adhesion of Silver Nanowires. *ACS Appl. Mater. Interfaces* **2013**, *5*, 9155−9160.

(12) Tuna, O.; Selamet, Y.; Aygun, G.; Ozyuzer, L. High Quality ITO Thin Films Grown by Dc and RF Sputtering without Oxygen. *J. Phys. D: Appl. Phys.* **2010**, *43*, 055402.

(13) David, S. H.; Richard, B. K. Solution-Processed Transparent Electrodes. *MRS Bull.* **2011**, *36*, 749−755.

(14) Yun, J.; Park, Y. H.; Bae, T. S.; Lee, S.; Lee, G. H. Fabrication of a Completely Transparent and Highly Flexible ITO Nanoparticle Electrode at Room Temperature. *ACS Appl. Mater. Interfaces* **2013**, *5*, 164−172.

(15) Wu, M. X.; Lin, X.; Wang, T. H.; Qiu, J. S.; Ma, T. L. Low-Cost Dye-Sensitized Solar Cell Based on Nine Kinds of Carbon Counter Electrodes. *Energy Environ. Sci.* **2011**, *4*, 2308−2315.

(16) Huang, S.; Li, L.; Yang, Z.; Zhang, L.; Saiyin, H.; Chen, T.; Peng, H. A New and General Fabrication of an Aligned Carbon Nanotube/Polymer Film for Electrode Applications. *Adv. Mater.* **2011**, *23*, 4707−4710.

(17) Yamaguchi, T.; Tobe, N.; Matsumoto, D.; Nagai, T.; Arakawa, H. Highly Efficient Plastic-Substrate Dye-Sensitized Solar Cells with Validated Conversion Efficiency of 7.6%. *Sol. Energy Mater. Sol. Cells* **2010**, *94*, 812−816.

(18) Lee, J.; Lee, S.; Li, G.; Petruska, M. A.; Paine, D. C.; Sun, S. A Facile Solution-Phase Approach to Transparent and Conducting ITO Nanocrystal Assemblies. *J. Am. Chem. Soc.* **2012**, *134*, 13410−13414.

(19) Dattoli, E. N.; Lu, W. ITO Nanowires and Nanoparticles for Transparent Films. *MRS Bull.* **2011**, *36*, 782−788.

(20) Puetz, J.; Aegerter, M. A. Direct Gravure Printing of Indium Tin Oxide Nanoparticle Patterns on Polymer Foils. *Thin Solid Films* **2008**, *516*, 4495−4501.

(21) Pasquarelli, R. M.; Ginley, D. S.; O'Hayrea, R. Solution Processing of Transparent Conductors: From Flask to Film. *Chem. Soc. Rev.* **2011**, *40*, 5406−5441.

(22) De, S.; Higgins, T. M.; Lyons, P. E.; Doherty, E. M.; Nirmalraj, P. N.; Blau, W. J.; Boland, J. J.; Coleman, J. N. Silver Nanowire Networks as Flexible, Transparent, Conducting Films: Extremely High DC to Optical Conductivity Ratios. *ACS Nano* **2009**, *3*, 1767−1774.

(23) Rathmell, A. R.; Bergin, S. M.; Hua, Y. L.; Li, Z. Y.; Wiley, B. J. The Growth Mechanism of Copper Nanowires and Their Properties in Flexible, Transparent Conducting Films. *Adv. Mater.* **2010**, *22*, 3558−3563.

(24) Tokuno, T.; Nogi, M.; Jiu, J.; Sugahara, T.; Suganuma, K. Transparent Electrodes Fabricated via the Self-Assembly of Silver Nanowires Using a Bubble Template. *Langmuir* **2012**, *28*, 9298−9302.

(25) Chen, S. P.; Kao, Z. K.; Lin, J. L.; Liao, Y. C. Silver Conductive Features on Flexible Substrates from a Thermally Accelerated Chain Reaction at Low Sintering Temperatures. *ACS Appl. Mater. Interfaces* **2012**, *4*, 7064−7068.

(26) Carlson, A.; Bowen, A. M.; Huang, Y. G.; Nuzzo, R. G.; Rogers, J. A. Transfer Printing Techniques for Materials Assembly and Micro/Nanodevice Fabrication. *Adv. Mater.* **2012**, *24*, 5284−5318.

(27) Lee, J.; Connor, S.; Cui, Y.; Peumans, P. Solution-Processed Metal Nanowire Mesh Transparent Electrodes. *Nano Lett.* **2008**, *8*, 689−692.

(28) Lee, K. S.; Lee, Y.; Lee, J. Y.; Ahn, J. H.; Park, J. H. Flexible and Platinum-Free Dye-Sensitized Solar Cells with Conducting-Polymer-Coated Graphene Counter Electrodes. *ChemSusChem* **2012**, *5*, 379−382.

(29) Wang, H.; Hu, Y. H. Graphene as a Counter Electrode Material for Dye-Sensitized Solar Cells. *Energy Environ. Sci.* **2012**, *5*, 8182−8188.

(30) Huang, Y. T.; Feng, S. P.; Chen, C. M. Nickel Substrate Covered with a Sn-Based Protection Bi-Layer as a Photoanode Substrate for Dye-Sensitized Solar Cells. *Electrochim. Acta* **2013**, *99*, 230−237.

(31) Feng, H. P.; Paudel, T. C.; Yu, B.; Chen, S.; Ren, Z. F.; Chen, G. Nanoparticle-Enabled Selective Electrodeposition. *Adv. Mater.* **2011**, *23*, 2454−2459.
(32) Ma, T.; Fang, X.; Akiyama, M.; Inoue, K.; Noma, H.; Abe, E. Properties of Several Types of Novel Counter Electrodes for Dye-Sensitized Solar Cells. *J. Electroanal. Chem.* **2004**, *574*, 77−83.
(33) Fang, X.; Ma, T.; Akiyama, M.; Guan, G.; Tsunematsu, S.; Abe, E. Flexible Counter Electrodes Based on Metal Sheet and Polymer Film for Dye-Sensitized Solar Cells. *Thin Solid Films* **2005**, *472*, 242−245.
(34) Bai, A.; Hu, C. C. Effects of Electroplating Variables on the Composition and Morphology of Nickel-Cobalt Deposits Plated through Means of Cyclic Voltammetry. *Electrochim. Acta* **2002**, *47*, 3447−3456.
(35) Kaganer, V. M.; Jenichen, B.; Shayduk, R.; Braun, W.; Riechert, H. Kinetic Optimum of Volmer-Weber Growth. *Phys. Rev. Lett.* **2009**, *102*, 016103.
(36) Khelladi, M. R.; Mentar, L.; Azizi, A.; Sahari, A.; Kahoul, A. Electrochemical Nucleation and Growth of Copper Deposition onto FTO and N-Si (100) Electrodes. *Mater. Chem. Phys.* **2009**, *115*, 385−390.
(37) Adriana, I.; Hisayoshi, M.; Andreas, B.; Benedetto, B. Nucleation and Growth of Thin Nickel Layers under the Influence of a Magnetic Field. *J. Electroanal. Chem.* **2009**, *626*, 174−182.
(38) Fu, N. Q.; Xiao, X. R.; Zhou, X. W.; Zhang, J. B.; Lin, Y. Electrodeposition of Platinum on Plastic Substrates as Counter Electrodes for Flexible Dye-Sensitized Solar Cells. *J. Phys. Chem. C* **2012**, *116*, 2850−2857.
(39) Chang, H.; Chen, T. L.; Huang, K. D.; Chien, S. H.; Hung, K. C. Fabrication of Highly Efficient Flexible Dye-Sensitized Solar Cells. *J. Alloys Compd.* **2010**, *504*, S435−S438.
(40) Kawashima, T.; Matsui, H.; Tanabe, N. New Transparent Conductive Films: FTO Coated ITO. *Thin Solid Films* **2003**, *445*, 241−244.
(41) Yin, X.; Xue, Z. S.; Liu, B. Electrophoretic Deposition of Pt Nanoparticles on Plastic Substrates as Counter Electrode for Flexible Dye-Sensitized Solar Cells. *J. Power Sources* **2011**, *196*, 2422−2426.
(42) Ikegami, M.; Miyoshi, K.; Miyasaka, T.; Teshima, K.; Wei, T. C.; Wan, C. C.; Wang, Y. Y. Platinum/Titanium Bilayer Deposited on Polymer Film as Efficient Counter Electrodes for Plastic Dye-Sensitized Solar Cells. *Appl. Phys. Lett.* **2007**, *90*, 153122.
(43) Lee, K. M.; Lee, E. S.; Yoo, B. Y.; Shin, D. H. Synthesis of ZnO-Decorated TiO_2 Nanotubes for Dye-Sensitized Solar Cells. *Electrochim. Acta* **2013**, *109*, 181−186.